Ecotoxicology and Environmental Safety 208 (2021) 111619

Contents lists available at ScienceDirect

Ecotoxicology and Environmental Safety

journal homepage: www.elsevier.com/locate/ecoenv

# Biodegradation of fluorene by the newly isolated marine-derived fungus, *Mucor irregularis* strain bpo1 using response surface methodology

Paul Olusegun Bankole [a,*,1], Kirk Taylor Semple [b], Byong-Hun Jeon [c], Sanjay Prabhu Govindwar [c]

[a] Department of Pure and Applied Botany, College of Biosciences, Federal University of Agriculture, P.M.B. 2240, Abeokuta, Ogun State, Nigeria
[b] Lancaster Environment Centre, Lancaster University, Lancaster LA1 4YQ, United Kingdom
[c] Department of Earth Resources and Environmental Engineering, Hanyang University, Seoul 04763, South Korea

ARTICLE INFO

Edited by Paul Sibley

*Keywords:*
*Mucor irregularis*
Polycyclic aromatic hydrocarbons
Fluorene
Biodegradation

ABSTRACT

Fluorene, a low molecular weight polycyclic aromatic hydrocarbon (PAH), is of immense environmental interest because of its carcinogenicity, teratogenicity, mutagenicity, toxicity and persistence to microbial degradation. Existentially, there is paucity of information on PAH degradation by fungi isolated from marine environment. Therefore, this study investigated fluorene degradation efficiency of marine derived filamentous fungus, *Mucor irregularis* strain bpo1 (GenBank Accession Number: MK373020). Response Surface Methodology (RSM) using Box–Behnken Design (BBD) was successfully deployed in the optimization of process parameters (pH-7, temperature-32.5 °C, substrate concentration-100 mg $L^{-1}$ and dry weight-2 g) resulting in 81.50% fluorene degradation on 5th day. The design and regression model were found to be statistically significant, adequate and appropriate with $p < 0.0001$, F value = 202.39, and predicted coefficient of determination ($R^2 = 0.9991$). Optimization of the vital constituents of the mineral salt medium (MSM) used for the study using RSM-Central Composite Design (CCD) resulted in 79.80% fluorene degradation rate. Enhanced fluorene degradation efficiency (82.50%) was recorded when the optimized process variables were subjected to growth-linked validation experiments. The enzyme activities revealed 87%, 59% and 31% induction of laccase, manganese peroxidase and lignin peroxidase respectively. Four metabolites; 9*H*-fluoren-9-one, benzene-1,2-dicarboxylic acid, 2-hydroxybenzoic acid and phenol obtained after the experiment were characterized and confirmed with GC-MS analysis. The findings revealed the promising potentials of *M. irregularis* in PAH degradation and by extension green remediation technology.

## 1. Introduction

Polycyclic aromatic hydrocarbons (PAHs) are a large group of organic chemicals composed of condensed aromatic rings (≥ 2) in linear, angular or clustered arrangements of cross-linked hydrogen and carbon atoms. Typically, PAHs are highly hydrophobic, less volatile and non-polar which makes them characteristically bioaccumulative in the environment (Johnsen et al., 2005). PAHs with four or more condensed aromatic rings are tagged as high molecular weight PAHs while the ones with four aromatic rings or less are referred to as low molecular weight (Haritash and Kaushik, 2009). Low molecular weight PAHs are water soluble with low melting and boiling points while high molecular weight PAHs less soluble in water with high melting and boiling points which makes them more stable, persistent, and arduous to break down during biodegradation (Patnaik, 2007). PAHs exhibit high tendency in accepting electrons and adherence to soil particles due poor water solubility (Tang and Krieger-Brockett, 2007). The constant surge in environmental pollution by PAHs is attributed to natural disasters like wild fires, volcanic eruptions and anthropogenic factors such as excessive use of fossil fuels as raw material by the industries (coal, petroleum, oil and gas). The enormity of PAHs in the environment raises grave environmental and health concerns due to their teratogenic, carcinogenic, toxigenic, and mutagenic effects. Their fate in the environment is dependent on volatilization, photo-oxidation, chemical oxidation, adsorption on soil particles, leaching and microbial degradation. Physical and chemical methods have been found to be expensive, energy-demanding and

* Corresponding author.
*E-mail address:* bankolepo@funaab.edu.ng (P.O. Bankole).
[1] ORCID: 0000-0003-3182-2990

https://doi.org/10.1016/j.ecoenv.2020.111619
Received 29 June 2020; Received in revised form 30 October 2020; Accepted 4 November 2020
Available online 13 November 2020

ineffective (Isaac et al., 2017). PAHs detoxification efficiency by fungi is a promising bioremediation alternative because it requires less energy, chemicals, and time (Czaplicki et al., 2018). However, the potency of fungi in the removal of PAHs in the environment is largely dependent on the strain and characteristics of organic pollutants (Al-Hawash et al., 2018). Several authors have reported biodegradation of vast majority of PAHs by fungi; phenanthrene by *Trametes hirsuta* (Hidayat and Yanto, 2018), anthracene by *Leucoagaricus gongylophorus* (Ike et al., 2019), benzo [a] pyrene by *Trichoderma asperellum* (Zafra et al., 2015), and pyrene by *Peniophora incarnata* (Lee et al., 2014).

The ability to secrete non-specific, non-selective extracellular enzymes confers on fungi the efficiency to breakdown diverse number of PAHs. To date, existential reports on PAH mineralization by non-white rot fungi are few and incomprehensive even though they are well adapted to high pollution impacted environments (Romero et al., 2010). Since Ahearn and Meyers (1972) reported PAH degradation efficiency by marine derived fungi, their application by other researchers has been poorly explored and investigated. Marine-derived fungi possesses saline tolerance features which makes them a good candidate for the bioremediation of polluted saline (Raghukumar et al., 2008) and an important precursor in their eco-friendly application in the remediation of PAH impacted environments (Haritash and Kaushik, 2009). The application of marine-derived fungi for the bioremediation of pollution impacted saline compartments is engineered by their tolerance to high saline conditions. These important features gave marine-derived fungi the edge in the remediation of PAH impacted saline environments (such as oceans and brackish sediments) (Birolli et al., 2018; Vieira et al., 2018). The National Waste Minimization Program which is saddled with the responsibility of reducing the usage and production of 31 priority chemicals enlisted fluorene to be teratogenic, carcinogenic, persistent and toxigenic in nature (EPA, 2016). Researchers are of the opinion that there is no safe level on the exposure of humans to fluorene which has over the years been tagged as a probable carcinogen. Fluorene has been implicated as a major cause of dysfunctional human reproductive system, lung, skin and liver cancer in animals.

Since there are few negligible reports of degradation of PAHs by marine fungi and the marine ecosystem is worst hit by PAH contamination, this present paper seeks to (1) investigate fluorene-degradation capacity of a filamentous isolated from marine soil (2) characterize the fungus using molecular sequence analysis (3) optimize physicochemical parameters and culture constituents using Response surface methodology-Box–Behnken Design (BBD) and Complete Composite Design (CCD) respectively for enhanced fluorene degradation (4) carry out extracellular enzyme activities to determine the influence of enzymes during degradation (5) characterize the metabolites using Gas-Chromatography Mass Spectrometry (GC-MS) analysis. To the best of our knowledge this is the first report on fluorene-degrading fungus isolated from marine soil. This study revealed the PAH biodegradation prowess of the new fungal strain.

## 2. Materials and methods

### 2.1. Chemicals

Fluorene (99.7%), potato dextrose agar, malt extract agar and HPLC grade methanol were procured from Sigma–Aldrich, UK. Dichloromethane, ethyl acetate, N′,N′-dimethylformamide (DMF), dimethylsulfoxide, acetone and other chemicals of high analytical grade and purity used were purchased from Merck (Darmstadt, Germany).

### 2.2. Sampling, microorganism and culture media

*Mucor irregularis* strain bpo1 was isolated from the soil collected from the shorelines of Atlantic Ocean, Lagos State, Nigeria (7°60′41″N; 4°09′19″E) using mineral salt medium (MSM) with addition of fluorene to a final concentration of 50 mg $L^{-1}$. The mixture was kept in a 250 mL Erlenmeyer flask at 29 °C for 7 days. The MSM was composed of 6.0 g $L^{-1}$ $KH_2PO_4$, 1.0 g $L^{-1}$ $Na_2SO_4$, 0.2 g $L^{-1}$ $MgSO_4{\cdot}7H_2O$, 0.05 g $L^{-1}$ yeast extract and 0.3 g $L^{-1}$ glucose. The mycelia biomass obtained was later centrifuged at x10,000*g* for 15 min. The fungus was thereafter maintained simultaneously in agar plates containing potato dextrose agar and nutrient broth composed of 20 g $L^{-1}$ glucose, 2 g $L^{-1}$ $KH_2PO_4$, 0.5 g $L^{-1}$ $MgSO_4{\cdot}7H_2O$, 0.1 g $L^{-1}$ $CaCl_2$, 0.2 g $L^{-1}$ yeast extract and 1000 mL of sterile distilled water and kept at a pH of 7 and at a temperature of 4 °C for further experimental use.

### 2.3. Molecular identification of fluorene degrading filamentous fungus strain

Total genomic DNA of *M. irregularis* strain bpo1 was extracted using cetyl-trimethylammonium bromide (CTAB) method as suggested by Griffith et al. (2009). The ITS 4 gene fragment was amplified by PCR using the forward primer ITS1F (5′ TCCGTAGGTGAACCTGCGG-3′) and reverse primer ITS4R (5′-TCCTCCGCTTATTGATATGC-3′). The polymerase chain reaction (PCR) conditions were as follows: initial denaturation at 94 °C for 5 min, 35 cycles at 94 °C for 30 s, at 55 °C for 35 s, and at 72 °C for 1 min, followed by a final extension at 72 °C for 8 min. Purified PCR products were sequenced at International Institute of Tropical Agriculture (IITA), Nigeria. Basic Local Alignment Search Tool (BLAST) query was used in confirming the identity of the nucleotides sequences on the National Centre for Biotechnology Information (NCBI) portal. The fungus strain molecular data were thereafter deposited on the portal for reference purpose. Sequence alignment was carried out in comparison with twenty-one (21) other similar and homologous sequences retrieved from NCBI portal using ClustalW facility on MEGA X Software (Kumar et al., 2018). Phylogenetic typing analyses were conducted using the neighbor-joining tree method (Tamura et al., 2004). Statistical support for the branching nodes was estimated using bootstrap values based on 500 replicates. The neighbor-joining tree represents the nucleotide sequences of the ITS gene and shows the relationships between *M. irregularis* (MK373020) strain bpo1 and 24 closely-related homologous taxa with accession numbers. The percentages at the nodes indicate the levels of bootstrap support based on the neighbor-joining analyses of the 500 resampling datasets.

### 2.4. Optimization of physicochemical parameters during fluorene degradation

Stock solution (100 mg $L^{-1}$) of fluorene was prepared by dissolving 0.005 g of fluorene in 50 mL ethyl acetate. The procedure was repeated for the preparation of other fluorene concentrations (200, 300, 400 and 500 mg $L^{-1}$). The degradation experiments were carried out in 500 mL-Erlenmeyer flasks containing 100 mL mineral salt medium (MSM). The media was supplemented with different concentrations (100–500 mg $L^{-1}$) of fluorene, mycelia dry weight (0.2–2.0 g). In addition, the incubation temperature was varied between (25–40 °C) while the pH of the medium was varied between 5 and 9 with the addition of HCl and NaOH to the mixture. Abiotic control was made of mixture with no fungus mycelia. The experimental set up were done in triplicates and kept for 5 days. Cultures were later filtered with Whatman filter paper to remove the solid and extract the fluorene in the mixture. The resultant fluorene present in the mixture after the experiment was extracted with ethyl acetate in ratio 30:70. The filtrate was thereafter dried overnight with $Na_2SO_4$. The absorbance of the filtrates (experimental and control) containing suspended solids were taken with HPLC machine (Shimadzu, Japan) at wavelength ($\lambda_{max}$ = 263 nm) (Bressler et al., 2000). Response surface methodology is a statistical sequential modeling technique used in establishing interactions between different variables with the aim of arriving at a given response. Typically, RSM is a full factorial mathematical enquiry which involves simultaneous and efficient variation of vital experimental conditions or parameters. A classical model is formed to test the interactive effect of the parameters with the aim of

determining the best conditions for optimal desired response (Das and Mishra, 2017). Prior to the study, a screening experiment was performed to determine the range of values of all the variable tested. In this study, Box–Behnken design (BBD) which is a class of rotatable three factorial second order design was deployed to determine the effect of important culture conditions; pH-5–9, temperature-25–40 °C, fluorene concentration-100–500 mg $L^{-1}$ (substrate), dry weight-0.2–2 g on the degradation efficiency of fluorene by *M. irregularis*. BBD is also deployed to study the interactions between the physicochemical variables.

Regression equation was derived from second order polynomials with experimental number of runs:

$$N = K^2 + K + C_P \quad (1)$$

Where $K$ (factor number) = 4 and $Cp$ (number of replications at the center point = 5) in the present study. The design model deployed was full quadratic which resulted in 25 experimental runs and analyzed using Design-expert software v. 12.0.1.0, Stat-Ease, Inc., Minneapolis, USA (Sutar et al., 2019). The experimental runs comprise of 22 trials and 3-center points with each run performed in triplicates and data were presented as mean ± standard error of means. The relationship between the coded and actual values is described as follows:

$$X_c = \frac{X_a - X_0}{\Delta X_f} \quad (2)$$

Where $X_c$ and $X_a$ are the coded and actual values of the independent variables respectively. $X_0$ is the actual value of the independent variable at the center point, and $\Delta X_f$is the step change of $X_a$. A second-degree polynomial was fitted to the experimental data to estimate the response of the dependent variable and predict the optimal point. The RSM-BBD experimental data on fluorene degradation was subjected to the analysis of variance (ANOVA) and fitted in second order polynomial (Eq. (3)). With full consideration of all terms, the quadratic response model is best represented as:

$$Y = b_0 + b_1A + b_2B + b_3C + b_4D + b_{12}AB + b_{13}BC + b_{23}AC + b_{34}AD + b_{23}BC + b_{34}BD + b_{14}CD + b_{11}A^2 + b_{22}B^2 + b_{33}C^2 + b_{44}D^2 \quad (3)$$

Where Y is predicted response, A, B, C and D are independent variables, $b_0$ is offset term, $b_1$, $b_2$, $b_3$, and $b_4$ are linear effects and $b_{11}$, $b_{22}$, $b_{33}$, and $b_{44}$ are squared terms and $b_{12}$, $b_{13}$, $b_{23}$, $b_{34}$, $b_{23}$, $b_{34}$ and $b_{14}$ interaction terms.

### 2.5. Optimization of fluorene degradation with variation in media components by RSM using CCD

Similarly, Central Composite Design (CCD) with five coded levels was used in determining the effect of vital medium components such as $KH_2PO_4$, $Na_2SO_4{\cdot}7H_2O$, $MgSO_4{\cdot}2H_2O$, yeast extract and glucose for optimal fluorene degradation. The five media components were studied at three alpha (α) levels (− 1, 0 and 1) with a set of 50 experiments. The five media components (A, B, C, D and E) were flagged as independent variables while percentage fluorene degradation represents the dependent response variable ($Y$) after a successful screening experiment (Ghevariya et al., 2011). Furthermore, the Central Composite Design (CCD) matrix was made of 4 axial points with 3 replicates and 3 center points (coded and actual values are given in Table 2) in order to enhance fluorene degradation. Percentage fluorene degradation (response $Y$) was explained as a second order response surface model Eq. (4) in five independent variables.

$$Y = \beta_0 + \Sigma\beta_i X_i + \quad \Sigma\beta_{ii} X^2{}_i + \Sigma\beta_{ij} X_i X_J \quad (4)$$

where $\beta_0, \beta_i, \beta_{ii}, \beta_{ij}$ represent respectively, the constant process effect between $X_i$ and $X_J$ on fluorene degradation process.

The combined effect of the above five parameters on fluorene degradation ranges as $KH_2PO_4$: 5–8 g $L^{-1}$, $Na_2SO_4{\cdot}7H_2O$: 1–3 g $L^{-1}$, $MgSO_4{\cdot}2H_2O$: 0.2–0.6 g $L^{-1}$, yeast extract: 0.05–0.15 g $L^{-1}$ and glucose: 0.1–0.3 g $L^{-1}$ was evaluated.

#### 2.5.1. Experimental validation of fluorene degradation using RSM model data

Fluorene degradation was experimentally validated with all optimized variables as obtained by RSM based on the data from the above sections. Simultaneously, fluorene degradation rate and growth of *M. irregularis* mycelia cells were taken at absorbance (wavelength - $\lambda_{max}$ = 560 nm). The results were juxtaposed with the confirmatory experiments done through enzyme induction, GC-MS and HPLC analyses (Xu and Lu, 2010).

### 2.6. Metabolites identification

#### 2.6.1. GC-MS analysis

The identification of the metabolites after fluorene degradation by *M. irregularis* was achieved using GC-MS technique. The fungus was inoculated and incubated in minimal salt medium (100 mL) in Erlenmeyer flask for 12 days with the addition of fluorene (200 mg $L^{-1}$) at 28 °C and 120 rpm. The biotic controls which contain no fungus was however made of equal volume of fluorene and kept under same culture conditions. The experimental assays were made in triplicates. Ethyl acetate was used as solvent in the adsorption of organic compounds and breakdown of grown mycelia cell biomass collected from the culture medium. Ethyl acetate (50 mL) was added to each flasks (experimental and control) and centrifuged at 10,000x*g* for 10 min. The resultant mixture was later filtered and transferred to a 250 mL separating funnel and shaken vigorously for 3 min. The organic phases were pooled together after two extractions and dried in vacuum using a rotary evaporator in a water bath at 30 °C. The resultant products were further dissolved in 2 mL of ethyl acetate where 1 mL was withdrawn and injected into the GC-MS system. The injected samples were separated in a GC system equipped with HP-5MS capillary column of dimension, 30 m × 0.25 mm × 0.25 m at an operating temperature of 60–280 °C. The temperature was elevated to 5 °C per minute and kept at 280 °C for 26 min, and from 280 °C to 310 °C, up 5 °C per minute and held at 310 °C for 5 min. The injector temperature was 250 °C (splitless injection) and the interface temperature was 300 °C. Samples were analyzed in Full Scan mode in the 50–600 $m/z$ range. Peaks were identified by comparing the mass spectrum and the data available in the library software NIST MS SEARCH version 2.0 and independently through fragmentation pattern interpretation. Metabolites were identified by one identification ion and at least one additional confirmation ion per compound, as mass spectra described in literature. Control experiments with no fluorene were equally analyzed.

#### 2.6.2. High performance liquid chromatography (HPLC) analysis

The resultant residue obtained in the procedure above (2.7.1) was dissolved in dichloromethane, diluted further in HPLC grade methanol and filtered. Residual fluorene was analyzed on HPLC machine (Shimadzu, Japan) using an ultraviolet detector with the absorbance set at 255 nm, 1.0 mL $min^{-1}$ flow rate and with a mobile phase made methanol and water in ratio 1.5:8.5. The retention times ($min^{-1}$) were thereafter observed and recorded.

### 2.7. Enzyme induction by M. irregularis during fluorene degradation

Induction of ligninolytic enzymes was studied from the experimental assays containing 100 mL of MSB, 200 mg $L^{-1}$ of fluorene, 7 mm disc of the fungal mycelia (Hadibarata and Kristanti, 2012). The biological control was set up alongside the experimental assay using the same substrate concentration without fungal mycelia. Both experimental and control assays were then incubated at 30 °C in a rotatory shaker incubator for 4, 8, 12, 16 and 20 days. All the experiments were performed in triplicates. Laccase activity was evaluated from the 3 mL sample

withdrawn from the mixture of enzyme extract (0.5 mL), sodium acetate buffer (1.5 mL) and guaiacol (1 mL). After a 2 h incubation, the absorbance was taken when the wavelength ($\lambda_{max}$ = 450 nm) sample. The laccase enzyme activity has been expressed in international units per liter of enzyme extract (U $L^{-1}$) (Sandhu and Arora, 1985).

Lignin peroxidase induction was determined from the reaction between culture filtrate (0.5 mL), sodium tartrate (1 mL), azure B (0.5 mL) and hydrogen peroxide (0.5 mL). Absorbance was read at 650 nm and expressed as 1 unit per liter (U $L^{-1}$) of the culture filtrate (Archibald, 1992). The reaction time was 30 min. Manganese peroxidase induction was evaluated from the sample (3 mL) taken in a mixture of culture filtrate (0.5 mL), sodium tartrate buffer (1 mL) and 2,6 DMP (1 mL). After 30 min, the activity was measured through the oxidation of 2,6 DMP with hydrogen peroxide (0.5 mL) at an absorbance wavelength of 470 nm and expressed as 1 unit per liter (U $L^{-1}$).

### 2.8. Statistical analysis

Response surface methodology and statistical analyses was performed by using Design Expert v.12.1.0.1 (Stat-Ease Inc., Minneapolis, USA). The obtained experimental data were analyzed using analysis of variance (ANOVA). All experiments were performed in triplicates and data were presented as mean ± standard error of means. The means were separated at $p < 0.05$ level of significance. A two-way Analyses of Variance (ANOVA) to determine normality and homogeneity of variances of the data enzymes induction and growth-linked validation experiment were conducted using Shapiro–Wilk and Levene statistic tests respectively with GraphPad Prism software version 8.4.2 (2020) at level of significance ($p \leq 0.05$).

## 3. Results and discussion

### 3.1. Identification and molecular characterization of M. irregularis strain bpo1

The molecular characterization of fungus strain through the Internal Transcribed Spacer (ITS) gene revealed its identity as *M. irregularis*. It was thereafter assigned an Accession Number (MK373020) upon submission of the NCBI portal using the BankIt tool. A full Basic Local Alignment Search Tool (BLAST) analysis of the fungus molecular sequence data revealed 91–100% homologous identity with 21 other sequences retrieved from the NCBI database. The evolutionary relationship with twenty-one (21) nucleotide sequences inferred through neighbor-joining tree method revealed that *M. irregularis* strain bpo1 belonged to the genus *Mucor* with close affinities to *M. irregularis* strain LZ04 (MN533717), *M. irregularis* strain LZ02 (MN533715), *M. irregularis* strain CMFCCCB (JX976255), *M. irregularis* strain CBS 700.71 (JN206154), *M. irregularis* strain URM7724 (MG269828), *M. irregularis* strain 607F12C-AM (MG751192), *M. irregularis* strain CBS 977.68 (JX976259) and *M. irregularis* strain CBS 977.68 (JN206155). The phylogenetic typing done through neighbor-joining method showed the relationship of the fungus with other sequences (Fig. 1).

### 3.2. Physicochemical parameters optimization for enhanced fluorene degradation using Box–Behnken method

Biodegradation of persistent organic pollutants is largely influenced by the concentration of the substrate, inoculum size, pH and incubation temperature. Hence, the present study was carried out to determine the effect of four different physicochemical parameters on fluorene degradation. Design expert v 12 was used in creating an experimental design with each parameter and their corresponding responses (Table 1). The second order polynomial coefficient (*Y*) for each response was determined through multiple linear regression. High degradation efficiency was observed at run 8 followed by 19, 1, 2, 17 and 6 with percentage degradation of 81.50%, 79.25%, 74.25%, 67.25%, 66.00% and 64.75% respectively. Same degradation efficiency (64.75%) was recorded at runs 6 and 16 which is as a result of similar experimental culture conditions. However, lowest degradation efficiency was recorded at runs 22, 7, 21 and 13 with percentage degradation of 23.50%, 27.25%, 31.25% and 35.00% respectively. The removal efficiency at run 1 with pH-5, temperature-32.5 °C, fluorene concentration-100 mg $L^{-1}$ and dry weight-1.1 g was 74.25%. Likewise, high fluorene degradation efficiency could be achieved at optimized culture conditions of pH-7, temperature-32.5 °C, fluorene concentration-100 mg $L^{-1}$, Dry weight-2 g. The optimized culture conditions favorable for maximum fluorene degradation obtained in this study were verified and validated at standard conditions.

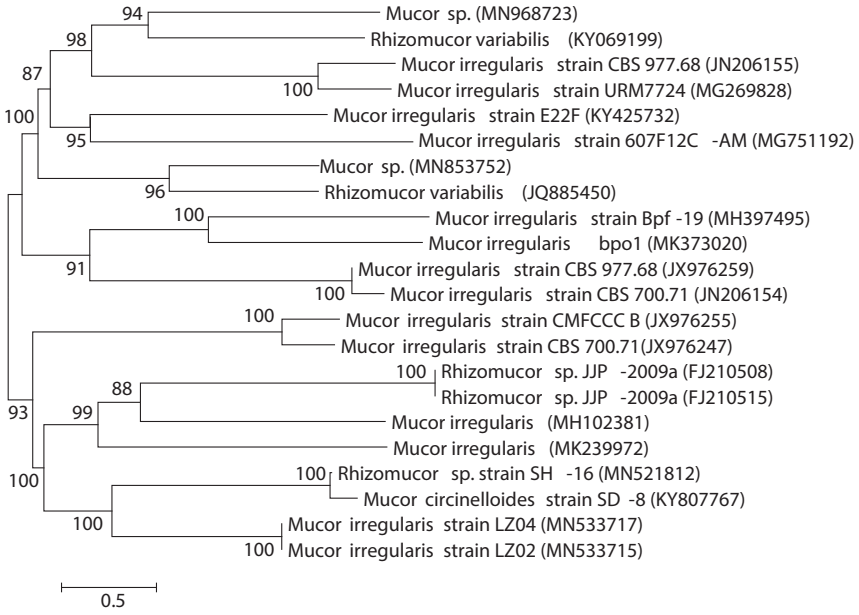


**Fig. 1.** Phylogenetic typing through neighbor-joining tree method of *M. irregularis* strain bpo1. The tree was inferred from analysis of sequence data with a scale bar of 0.50 indicating the genetic distance.

**Table 1**
Box–Behnken design for the degradation of fluorene by *M. irregularis*.

| Run no. | pH | | Temperature (°C) | | Substrate | | Dry weight (g) | | Degradation efficiency (%) | |
|---|---|---|---|---|---|---|---|---|---|---|
| | Coded | Actual | Coded | Actual | Coded | Actual | Coded | Actual | Experimental | Predicted |
| 1 | 1 | 5 | 0 | 32.5 | −1 | 100 | 0 | 1.1 | 74.25 | 73.93 |
| 2 | 0 | 7 | 1 | 40 | −1 | 100 | 0 | 1.1 | 67.25 | 68.70 |
| 3 | −1 | 5 | 0 | 32.5 | 0 | 300 | −1 | 0.2 | 41.50 | 40.22 |
| 4 | 0 | 7 | 1 | 40 | 0 | 300 | −1 | 0.2 | 44.75 | 45.12 |
| 5 | 0 | 7 | −1 | 25 | −1 | 100 | 0 | 1.1 | 63.50 | 64.01 |
| 6 | 0 | 7 | 0 | 32.5 | 1 | 500 | −1 | 0.2 | 64.75 | 63.93 |
| 7 | −1 | 5 | 1 | 40 | 0 | 300 | 0 | 1.1 | 27.25 | 27.41 |
| 8 | 0 | 7 | 0 | 32.5 | −1 | 100 | −1 | 0.2 | 81.50 | 80.98 |
| 9 | 1 | 9 | 0 | 32.5 | 0 | 300 | −1 | 0.2 | 49.25 | 48.77 |
| 10 | −1 | 5 | 0 | 32.5 | 1 | 500 | 0 | 1.1 | 47.25 | 47.88 |
| 11 | 0 | 7 | −1 | 40 | 0 | 300 | 1 | 2 | 42.50 | 41.99 |
| 12 | 1 | 9 | 0 | 32.5 | 1 | 500 | 0 | 1.1 | 55.00 | 55.09 |
| 13 | 1 | 9 | 1 | 40 | 0 | 300 | 0 | 1.1 | 35.00 | 34.92 |
| 14 | 0 | 7 | −1 | 25 | 0 | 300 | −1 | 0.2 | 41.00 | 39.07 |
| 15 | 0 | 7 | −1 | 25 | 1 | 500 | 0 | 1.1 | 46.75 | 47.02 |
| 16 | 0 | 7 | 0 | 32.5 | 1 | 500 | 1 | 2 | 64.75 | 65.47 |
| 17 | 0 | 7 | 0 | 32.5 | 0 | 300 | 0 | 1.1 | 66.00 | 59.66 |
| 18 | −1 | 5 | 0 | 32.5 | 0 | 300 | 1 | 2 | 39.25 | 39.33 |
| 19 | 0 | 7 | 0 | 32.5 | −1 | 100 | 1 | 2 | 79.25 | 80.05 |
| 20 | −1 | 5 | 0 | 32.5 | −1 | 100 | 0 | 1.1 | 64.00 | 63.87 |
| 21 | 1 | 9 | −1 | 25 | 0 | 300 | 0 | 1.1 | 31.25 | 30.90 |
| 22 | −1 | 5 | −1 | 25 | 0 | 300 | 0 | 1.1 | 23.50 | 23.57 |
| 23 | 0 | 7 | −1 | 25 | 0 | 300 | 1 | 2 | 38.75 | 38.92 |
| 24 | 1 | 9 | 0 | 32.5 | 0 | 300 | 1 | 2 | 47.00 | 46.88 |
| 25 | 0 | 7 | 1 | 40 | 0 | 500 | 0 | 1.1 | 50.50 | 50.91 |
| 26 (Control) | – | – | – | – | – | – | – | – | – | – |

### 3.2.1. Model adequacy, fitting of second-order polynomial equation and statistical analysis

The ANOVA (Table SM1) for the full quadratic, non-aliased model showed that the design model is very significant and sufficient for the experiment with F-value (202.39) and a corresponding p-value ($< 0.0001$) (Table SM1). The findings further suggest that there is 0.0001% chance for a F-value this large could occur as a result of noise. The p-value (x) must obey $0.05 \leq x \leq 0.1$, hence the model would be regarded as insignificant. The F-value further implied an insignificant difference between the center and factorial points in the design matrix which ensures goodness of fit and use of model. Moreover, the "lack of fit" F-value for the model is 3.04 which signifies its insignificance relative to pure error. The "lack of fit p-value" of this model indicates that there is 95.60% chance of no-significant lack of fit which is good enough for the model. In addition, results obtained in Table SM1 and Fig. 2e revealed that the Cook's distance has no outlier points (D) above 1 which suggests goodness of fit of the model. The coefficient of variation (C.V) which is the ratio of the mean to the standard error of means of observed responses. In this study, the C.V is 1.40 which is far $< 10\%$ indicates the reliability and reproducibility of the model. Low standard deviation of 0.719 indicates a high level of accuracy and an excellent consistency of the model for the experimental results (Table SM2). For a good degree of fitness, the coefficient of determination ($R^2$) which is the ratio of observed variation and total variation, should be $\geq 0.8$. The R-squared value obtained using this model was 0.9991 which showed high degree of correlation between predicted and experimental fluorene degradation efficiencies. Also, the marginal difference between predicted $R^2$ (0.9991) and adjusted $R^2$ (0.9980) is far less than 0.2 which suggests model adequacy and that there was no problem encountered during the experiment, data analysis and model design. The adjusted $R^2$ further affirmed that the accuracy of the model predicted response could be 99.80% and that the prediction of experimental data is quite satisfactory. In this study, the adequate precision which is the ratio of signal to noise was 106.106 (Table SM2). This signifies that the fluorene degradation efficiency has adequate signal since the adequate precision if far $> 4$. Therefore, provisionally quadratic model was chosen for further analysis.

The equation in terms of coded factors

$$Fluorenedegradationefficiency(\%) = 66.00 + 4.08A + 1.88B + 8.40C - 0.9375D + 0.0002AB - 0.6250AC + 0.0001AD + 0.0003BC + 0.0001BD + 0.5625CD - 17.01A^2 - 19.82B^2 + 11.02C^2 - 4.54D^2 \quad (5)$$

Table SM3 represents the estimated coefficients of corresponding parameter alongside variance inflation factor (VIF), confidence limits and standard error. The VIF value for all process parameters is 1 which connotes the magnitude of multi-collinearity in the regression analysis (Mishra and Maiti, 2019). While other process parameters how positive coefficients in the model, negative coefficients (− 8.40 and − 0.9375) were obtained for factors C (substrate concentration) and D (dry weight) respectively. The negative coefficient values of concentration and dry weight is due to the large influence exerted by the parameters above others during fluorene degradation by *M. irregularis* (Mishra and Maiti, 2019). The Eq. (5) represents coded factors which is typically used in making response variable ($Y$) predictions for each process variables having high and low levels as + 1 and − 1 respectively. A match to model design value was observed in the Box-Cox plot for power transformation (Fig. SM1c) where the minimum and maximum lambda values are 0.82 and 1.13 respectively. The finding further suggest that transformation is absolutely needless for model fitting in getting the response variable. In addition, the leverage versus run plot revealed that the variable and numerical data falls within the standard limits of 0–1 of an experimental trial (Fig. SM1d) which affirmed that the design points do not distort the fitness, relevance and appropriateness of the model. The Cook's distances plot is used in elucidating response outlier for corresponding experimental trial (Fig. SM1e). In this study, the Cook's distance values obtained are $< 1$ which is indicative of the normal distribution and constant variance of the residuals. Furthermore, the value of cook's distances affirmed that there were no outliers for the response data. Steep slopes indicating high sensitivity to the fluorene degradation efficiency ($Y$) variable were obtained in the perturbation plot (Fig. SM1) representing the interaction effect of process variables on performance of the system. Out of all the process parameters, slope of substrate concentration (C) is steeper followed by parameter D and A, confirmed its high sensitivity on the fluorene degradation percentage (response)

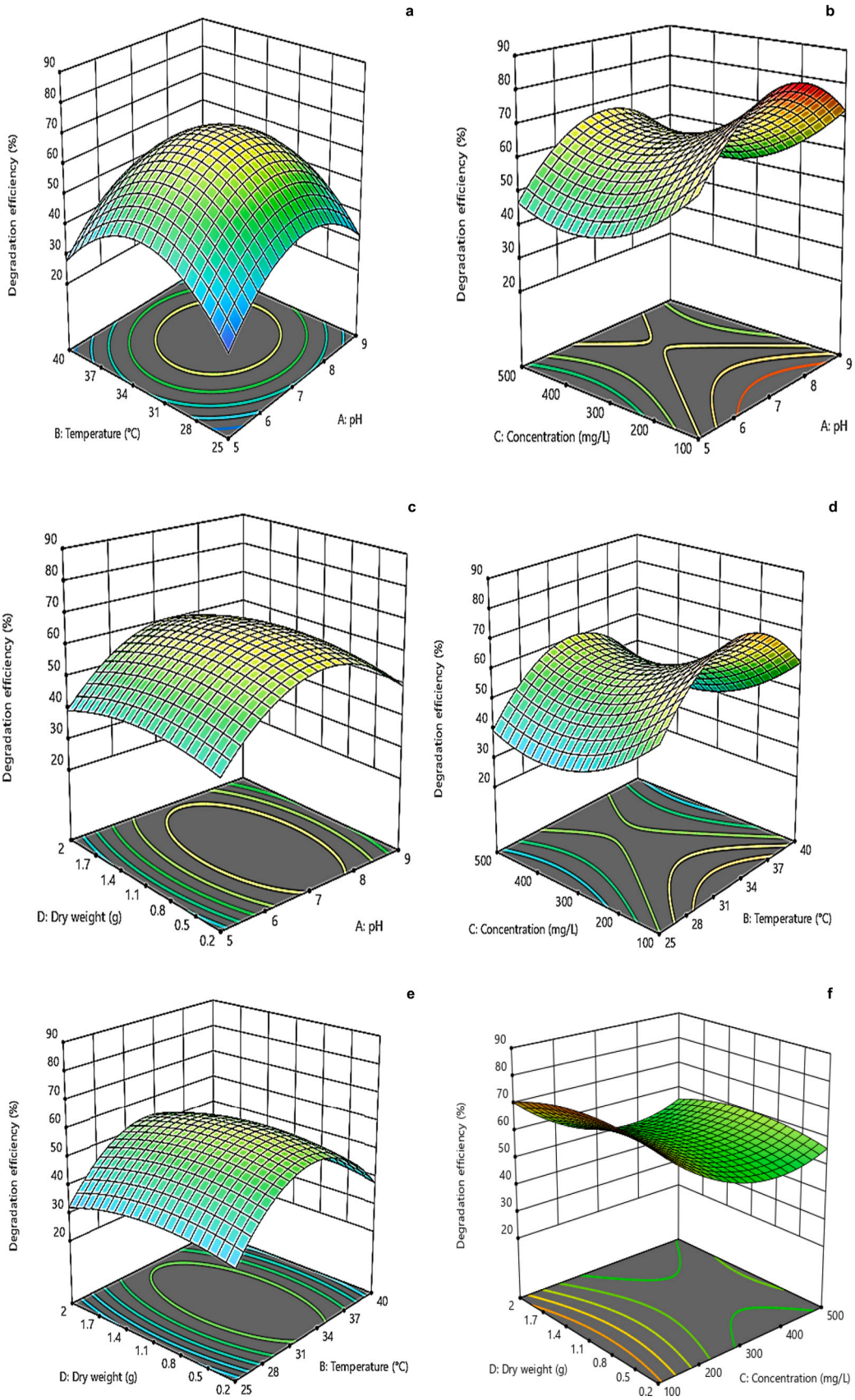


**Fig. 2.** Surface and contour plots of fluorene degradation efficiency (%): (a) effect of pH and temperature; (b) effect of concentration and pH; (c) effect of pH and dry weight; (d) effect of concentration and temperature; (e) effect of temperature and dry weight; (f) effect of concentration and dry weight.

than others.

### 3.2.2. Optimization of process variables on fluorene degradation efficiency by M. irregularis

Interaction effects and optimal levels of the variables were determined by plotting the response surface contour plots (Fig. 2) which showed the behavior of response (% fluorene degradation efficiency) with respect to simultaneous change in two variables. The multiple regression plot is typically elucidated by three-dimensional (3D) mesh response plots in process optimization with RSM. The relationship between fluorene degradation efficiency (dependent variable) and other four process parameters-independent variables (pH, temperature, substrate concentration and dry weight) are presented in 3D surface plots with their contour plots (Fig. 2). While other variables are kept constant at fixed level, the individual plots represent the effect of two independent process variable on fluorene degradation efficiency by *M. irregularis*. The degree of interactions between two process parameters could be depicted from nature of contour plots. An oval contour plot indicates close interaction while a circular contour plot suggests negligible interaction between two variables. Fig. 2a showed the interaction effect of pH and temperature on fluorene degradation rate. As seen on the 3D mesh plot, the spherical surface implies that there is a local maximum region under certain ranges of pH and temperature. In addition, an increase in pH and dry weight initially led to increase in fluorene degradation rate. The optimal level of pH and temperature were 7 and 32.5 °C respectively for maximum degradation of fluorene (62.1%). Additionally, pH and ionic strength of water phase also affect its state which in turn allows effective biodegradation of targeted organic pollutant (Sandrin and Maier, 2003). The 3D mesh and contour plots (Fig. 2b) shows the interactive effect of concentration and pH on fluorene degradation efficiency. The ellipsoidal nature of the shape indicates decrease in degradation efficiency at concentrations ranging between 100 and 500 mg $L^{-1}$. Ultimately, maximum degradation efficiency 81.5% was achieved at a pH 7.2 and concentration (100 mg $L^{-1}$). Further increases in both variables above 32.5 °C and 100 mg $L^{-1}$ resulted in decrease in degradation rate of fluorene. The concentration of substrate plays a significant role in degradation efficiency. The higher the concentration, the higher the toxicity of PAH metabolites and distortion of the degradation system (Kim et al., 2005). Similarly, the elliptical and contour plots in Fig. 2c showed that the maximum percentage degradation of fluorene (60.6%) was achieved at pH 7 and dry weight (1.1 g). Fungi perform optimally at a pH range 5–7. Although, a high fluorene degradation rate was favored with increasing dry weight however a further increase in pH led to decrease in fluorene degradation efficiency. The sinusoidal 3D mesh plot showing interactive effect of temperature and concentration (Fig. 2d) revealed maximum degradation rate (71.1%) when the temperature and concentration were 32.5 °C and 100 mg $L^{-1}$ respectively. Lowest degradation efficiency was however recorded when the temperature and concentration was set above 35 °C and 200 mg $L^{-1}$ of fluorene respectively. Typically, lower concentrations and ambient temperature usually favors maximum degradation of PAHs. An increase in fluorene concentrations from 200 to 500 mg $L^{-1}$ resulted in sharp decline in degradation efficiency to about 47.25%. This indicates that *M. irregularis* is a mesophilic fungus which grows best at room temperature. At a much higher temperature above ambience, the mycelia cells experiences apoptosis (cell death) and in turn loses the efficiency in effective degradation of PAHs. Furthermore, most filamentous fungi thrive and proliferates best at temperature range of 25–35 °C (Fu and Viraraghavan, 2001). The elliptical shape obtained from the interaction between dry weight and temperature (Fig. 2e) show that maximum degradation (60.0%) which further suggest significant quadratic effect of the two process variables. Fig. 2f shows the interactive effect of dry weight and concentration on fluorene degradation rate. It was evident that maximum degradation of fluorene (75.2%) was achieved at dry weight (1.1 g) and concentration (100 mg $L^{-1}$). The finding corroborated earlier work by Abdelhay et al. (2008) which reported higher phenanthrene degradation rate on increase in inoculum size.

### 3.2.3. Optimization of media components by RSM using CCD

Eq. (6) depict a quadratic relationship between fluorene degradation efficiency (*Y*)-dependent variable and vital media components-independent variables. From Table 2 which represents the CCD, it is clear that there were close matches between the predicted and experimental values during fluorene degradation by *M. irregularis*. The Fisher's (F-value) (33.26) obtained from the ANOVA was found to be high (Table SM5) which affirmed that the likely variations in response factor (fluorene degradation percentage) would be well catered for by the regression model equation. The p value obtained in this study is $< 0.0001$ which suggests that the model is statistically significant at $> 95\%$ confidence interval. In addition, the linear and square terms of the regression model for fluorene degradation on 5th day were found highly significant ($p < 0.0001$). Furthermore, the interaction between independent parameters were also found to be statistically relevant at 95% confidence level. Overall, the regression model was statistically significant ($p < 0.0001$) which connotes that the second order polynomial was appropriate and adequate for determining the actual relationship between fluorene degradation percentage (*Y*) and media components (process variables-A, B, C, D and E). The ANOVA revealed significant interaction between the variables. The regression coefficient of determination ($R^2 = 0.9582$), predicted $R^2$ (0.8518) and adjusted $R^2$ (0.9294) indicated that the model is highly reliable on reproducibility of experiments by other researchers (Table SM4). The second order RSM equally revealed the quadratic and interaction effects of the media constituents in relation to fluorene degradation rate. The coefficient for the linear effect of $KH_2PO_4$ ($p < 0.0001$), $Na_2SO_4$ ($p < 0.0001$), $MgSO_4$ ($p < 0.0001$), yeast extract ($p < 0.0001$), and ($p < 0.0001$) were highly significant. The interaction between A: $KH_2PO_4$ and B: $Na_2SO_4$ ($p = 0.0140$), A: $KH_2PO_4$ and D: yeast extract ($p = 0.0227$), A: $KH_2PO_4$ and E: glucose ($p = 0.0364$), B: $Na_2SO_4$ and C: $MgSO_4$ ($p = 0.0174$), B: $Na_2SO_4$ and D: yeast extract ($p = 0.0021$), C: $MgSO_4$ and D: yeast extract ($p = 0.0177$) and D: yeast extract and E: glucose ($p = 0.0047$) were statistically significant (Table SM5). The fitted second order response surface model specified by Eq. (6) for percent degradation of fluorene in coded process variables is:

$$\begin{aligned} Y = 20.92 - 8.93A - 7.24B - 5.79C - 6.45D - 6.33E - 0.1969AB \quad + 0.8031AC \\ -1.49AD + 1.47AE + 0.3531BC + 0.7844BD - 0.8031BE \\ -0.2156CD + 0.1969CE + 0.4906DE + 6.37A^2 + 7.46B^2 - 2.14C^2 + 2.69D^2 + 9.66E^2 \end{aligned} \quad (6)$$

### 3.2.4. Effect of interaction between the media components on fluorene degradation

Fig. SM1 represents contour plots for degradation of fluorene by *M. irregularis* on 5th day as observed after a number of repeated experiments. Each contour plot represents a number of combinations of two test variables with the other variable maintained at zero level. The maximum percent degradation of fluorene is indicated on the surface of the contour plot (Fig. SM2). Studies of the contour plots also reveal the

**Table 2**
Full factorial CCD of vital media constituents for fluorene degradation by *M. irregularis*.

| Run no. | $KH_2PO_4$ | | $Na_2SO_4$ | | $MgSO_4$ | | Yeast extract | | Glucose | | Degradation efficiency (%) | |
|---|---|---|---|---|---|---|---|---|---|---|---|---|
| | Coded | Actual | Coded | Actual | Coded | Actual | Coded | Actual | Coded | Actual | Experimental | Predicted |
| 1 | 1 | 8 | −1 | 1 | 1 | 0.6 | 1 | 0.15 | −1 | 0.1 | 27.00 | 27.05 |
| 2 | 1 | 8 | 1 | 3 | 1 | 0.6 | −1 | 0.05 | 1 | 0.3 | 23.00 | 22.87 |
| 3 | 1 | 8 | 1 | 3 | −1 | 0.2 | 1 | 0.15 | −1 | 0.1 | 22.20 | 22.25 |
| 4 | 1 | 8 | −1 | 1 | 1 | 0.6 | −1 | 0.05 | 1 | 0.3 | 39.00 | 38.86 |
| 5 | 0 | 6.5 | 0 | 2 | 0 | 0.4 | 0 | 0.1 | 0 | 0.2 | 19.20 | 19.00 |
| 6 | −1 | 5 | −1 | 1 | −1 | 0.2 | −1 | 0.05 | −1 | 0.1 | 79.80 | 80.00 |
| 7 | 0 | 6.5 | 0 | 2 | 0 | 0.4 | 0 | 0.1 | 0 | 0.2 | 29.60 | 29.51 |
| 8 | −1 | 5 | −1 | 1 | 1 | 0.6 | 1 | 0.15 | 1 | 0.3 | 42.00 | 41.13 |
| 9 | −1 | 5 | 1 | 3 | 1 | 0.6 | −1 | 0.05 | 1 | 0.3 | 38.00 | 38.03 |
| 10 | 0 | 6.5 | 0 | 2 | −1 | 0.2 | 0 | 0.1 | 0 | 0.2 | 25.00 | 25.41 |
| 11 | 1 | 8 | −1 | 1 | −1 | 0.2 | −1 | 0.05 | −1 | 0.1 | 64.80 | 65.01 |
| 12 | 0 | 6.5 | 0 | 2 | 0 | 0.4 | 1 | 0.15 | 0 | 0.2 | 18.40 | 18.84 |
| 13 | 0 | 6.5 | 0 | 2 | 0 | 0.4 | 0 | 0.1 | −1 | 0.1 | 29.60 | 29.01 |
| 14 | −1 | 5 | 1 | 3 | −1 | 0.2 | −1 | 0.05 | 1 | 0.3 | 49.20 | 48.93 |
| 15 | −1 | 5 | 1 | 3 | −1 | 0.2 | −1 | 0.05 | −1 | 0.1 | 63.80 | 63.00 |
| 16 | −1 | 5 | 1 | 3 | −1 | 0.2 | 1 | 0.15 | 1 | 0.3 | 37.20 | 37.25 |
| 17 | −1 | 5 | −1 | 1 | −1 | 0.2 | −1 | 0.05 | 1 | 0.3 | 65.20 | 65.00 |
| 18 | −1 | 5 | −1 | 1 | 1 | 0.6 | −1 | 0.05 | 1 | 0.3 | 54.00 | 53.86 |
| 19 | 0 | 6.5 | 0 | 2 | 0 | 0.4 | 0 | 0.1 | 0 | 0.2 | 19.20 | 19.00 |
| 20 | 1 | 8 | 1 | 3 | 1 | 0.6 | 1 | 0.15 | −1 | 0.1 | 29.20 | 28.97 |
| 21 | 1 | 8 | 1 | 3 | −1 | 0.2 | −1 | 0.05 | 1 | 0.3 | 34.20 | 34.10 |
| 22 | −1 | 5 | −1 | 1 | 1 | 0.6 | 1 | 0.15 | −1 | 0.1 | 56.60 | 56.51 |
| 23 | 1 | 8 | −1 | 1 | −1 | 0.2 | 1 | 0.15 | 1 | 0.3 | 38.20 | 38.01 |
| 24 | −1 | 5 | 1 | 3 | 1 | 0.6 | 1 | 0.15 | −1 | 0.1 | 40.60 | 40.54 |
| 25 | 0 | 6.5 | 0 | 2 | 0 | 0.4 | 0 | 0.1 | 0 | 0.2 | 21.00 | 20.89 |
| 26 | 1 | 8 | −1 | 1 | 1 | 0.6 | 1 | 0.15 | −1 | 0.3 | 27.00 | 26.88 |
| 27 | 0 | 6.5 | 0 | 2 | 0 | 0.4 | 0 | 0.1 | 0 | 0.2 | 19.20 | 18.97 |
| 28 | 0 | 6.5 | 0 | 2 | 0 | 0.4 | 0 | 0.1 | 0 | 0.2 | 19.20 | 19.05 |
| 29 | 0 | 6.5 | 0 | 2 | 0 | 0.4 | 0 | 0.1 | 0 | 0.2 | 19.20 | 18.99 |
| 30 | 0 | 6.5 | 0 | 2 | 1 | 0.6 | 0 | 0.1 | 0 | 0.2 | 13.80 | 13.96 |
| 31 | −1 | 5 | −1 | 1 | 1 | 0.6 | −1 | 0.05 | −1 | 0.1 | 68.60 | 69.05 |
| 32 | 0 | 6.5 | 0 | 2 | 0 | 0.4 | 0 | 0.1 | 0 | 0.2 | 19.20 | 19.00 |
| 33 | 0 | 6.5 | 0 | 2 | 0 | 0.4 | 0 | 0.1 | 0 | 0.2 | 19.20 | 19.98 |
| 34 | −1 | 5 | 1 | 3 | 1 | 0.6 | 1 | 0.15 | 1 | 0.3 | 26.00 | 25.76 |
| 35 | 1 | 8 | 1 | 3 | 1 | 0.6 | −1 | 0.05 | −1 | 0.1 | 37.90 | 38.00 |
| 36 | −1 | 5 | −1 | 1 | −1 | 0.2 | 1 | 0.15 | 1 | 0.3 | 53.20 | 53.89 |
| 37 | −1 | 5 | 1 | 3 | 1 | 0.6 | −1 | 0.05 | −1 | 0.1 | 52.60 | 52.01 |
| 38 | 1 | 8 | 0 | 2 | 0 | 0.4 | 0 | 0.1 | 0 | 0.2 | 19.60 | 20.00 |
| 39 | 1 | 8 | 1 | 3 | −1 | 0.2 | 1 | 0.15 | 1 | 0.3 | 22.20 | 22.28 |
| 40 | −1 | 5 | −1 | 1 | −1 | 0.2 | 1 | 0.15 | −1 | 0.1 | 67.80 | 66.50 |
| 41 | 1 | 8 | 1 | 3 | 1 | 0.6 | 1 | 0.15 | 1 | 0.3 | 11.00 | 11.33 |
| 42 | 0 | 6.5 | −1 | 1 | 0 | 0.4 | 0 | 0.1 | −1 | 0.2 | 37.00 | 36.72 |
| 43 | 1 | 8 | −1 | 1 | −1 | 0.2 | −1 | 0.05 | 1 | 0.3 | 50.20 | 51.65 |
| 44 | 0 | 6.5 | 0 | 2 | 0 | 0.4 | 0 | 0.1 | 1 | 0.3 | 32.80 | 31.99 |
| 45 | 1 | 8 | 1 | 3 | −1 | 0.2 | −1 | 0.05 | −1 | 0.1 | 48.80 | 49.01 |
| 46 | 0 | 6.5 | 1 | 3 | 0 | 0.4 | 0 | 0.1 | 0 | 0.2 | 21.00 | 20.87 |
| 47 | 1 | 8 | −1 | 1 | −1 | 0.2 | 1 | 0.15 | −1 | 0.1 | 47.00 | 46.88 |
| 48 | 0 | 6.5 | 0 | 2 | 0 | 0.4 | 0 | 0.1 | 0 | 0.2 | 19.20 | 20.12 |
| 49 | −1 | 5 | 1 | 3 | −1 | 0.2 | 1 | 0.15 | −1 | 0.1 | 67.80 | 68.03 |
| 50 | 1 | 8 | −1 | 1 | 1 | 0.6 | −1 | 0.05 | −1 | 0.1 | 53.60 | 52.89 |

best optimum value of the process conditions as $KH_2PO_4$ – 5.0 g $L^{-1}$, $Na_2SO_4$ – 1.00 g $L^{-1}$, $MgSO_4$ – 0.20 g $L^{-1}$, yeast – 0.05 g $L^{-1}$ and glucose – 0.1 g $L^{-1}$. The maximum degradation rate recorded at the best optimum media condition was 79.80% while the lowest fluorene degradation rate was 11.00% when $KH_2PO_4$, $Na_2SO_4$, $MgSO_4$, yeast and glucose were 8, 3, 0.6, 0.15 and 0.3 g $L^{-1}$ respectively. The actual proportions of $KH_2PO_4$, $Na_2SO_4$, MgSO4, yeast extract and glucose prior to experimentation were 6.0, 1.0, 0.2, 0.05 and 0.3 g $L^{-1}$ respectively. The results of this study were however in disagreement with previous similar work by Bhatt et al. (2014) which reported enhanced degradation of chrysene with 0.1 g $L^{-1}$ $MgSO_4$ and 0.5 g $L^{-1}$ $KH_2PO_4$ albeit low degradation efficiency (46.67%). $Na^{2+}$ ions play a vital role in membrane mechanisms and cultures involving degradation of PAHs by fungi. Being enzyme co-factors, metal ions such as $Mg^{2+}$ helps in enhancing proliferation of microbial mycelia cells and invariably improve degradation efficiency (Santos et al., 2008). The addition of readily utilizable carbon source (i.e. glucose as a co-substrate) is considered as an alternative to promote biodegradation resulting in an increase in biomass thereby increasing growth linked degradative ability of the isolate (Simarro et al., 2012). Similar results have also been reported by Hadibarata and Tachibana and Bhatt et al., (2009, 2014) with 65% and 76.35% of chrysene removal by a white rot fungus *Polyporus* sp. S133 and *Armillaria* sp. respectively. Increased addition of glucose in the degradation set leads to over saturation which in turn distorts bioremediation efficiency (Mohana et al., 2008). Hence, a proper choice of level combination of glucose is desirable for enhancing PAH degradation. Thus, addition of inorganic nutrients increased mineralization and shortened adaptation periods.

### 3.3. Determination of metabolic fate with GC-MS and HPLC analyses

Four metabolites were obtained during the fluorene degradation by *M. irregularis* (Table SM6). The identity of four of the metabolites were confirmed with other spectra obtainable in the GC-MS library. The first

metabolite; 9*H*-fluoren-9-one (mw = 180.20 g mol$^{-1}$, $m/z = 181$) at $R_t$ = 33.08 min was as a result of partial decarboxylation of the cyclopentene ring of the fused fluorene structure (Table SM6). The second metabolite was formed as a result dual carboxylation of one of the benzene aromatic ring which led to the formation of benzene-1,2-dicarboxylic acid (mw = 166.13 g mol$^{-1}$, $m/z = 166$) at $R_t$ = 19.54 min. Loss of hydroxyl compounds and further reduction of benzene-1,2-dicarboxylic acid resulted in an organic acid (2-hydroxybenzoic acid) of lower molecular weight (mw = 138.12, $m/z = 138$) at $R_t$ = 14.67 min. The final metabolite, phenol (mw = 94.11, $m/z = 95$) was formed as a result of decarboxylation of the benzoic acid at $R_t$ = 10.19 min (Table SM6, Fig. SM3). It is however noteworthy to state that this is the first report on the biodegradation of fluorene which resulted in the final product, phenol. Multiple peaks shown elucidated on the GC-MS spectra were due to the action of extracellular enzymes secreted by *M. irregularis*. Non-stereo selective enzymes deployed by fungi during biodegradation of organic pollutants have been implicated in the ring cleavage, asymmetric cleavage, oxidation, demethylation, desulfonation, oxidation, carboxylation and decarboxylation processes leading to their breakdown. Most existential works in literature by previous researchers reported the oxidation of fluorene by different species of fungi to metabolites of high molecular weights-9-fluorenol, 9-fluorenone, and 2-hydroxy-9-fluorenone (Johannes and Majcherczyk, 2000). However, the fungus used in this study was able to degrade fluorene to phenol which is of lower molecular weight. The formation of these metabolites was engineered by the activities of enzymes produced by the fungus during degradation. This study was able to ascertain the specific enzymes responsible for decarboxylation, carboxylation, ring and asymmetric cleavages of the metabolites. However, the transformation, decarboxylation and polymerization of most phenolic, non-phenolic and aromatic compounds through oxidation is attributed to the action of laccases and lignin peroxidases which are non-selective and non-specific (Crampon et al., 2014). Furthermore, LiP, Lac and MnP has been implicated in the degradation of several PAHs to less toxic metabolites (Bogan and Lamar, 1995). HPLC spectrum of the untreated fluorene (data not shown) revealed peaks at retention times ($R_t$) 1.327 and 1.412 min (Fig. SM4a, Table SM7). The metabolites obtained on treatment of fluorene with *M. irregularis* resulted in four (4) distinct peaks at retention times ($R_t$ = 1.431, 1.489, 1.553 and 1.607 min) (Fig. SM4b).

### 3.4. Enzyme analyses

Efficient and enhanced degradation of PAH by fungi is usually aided through optimum induction of extracellular enzymes. Therefore, enzyme assay activities were carried out during fluorene removal by *M. irregularis* in comparison with their biotic controls (Fig. 3). Lac (1663.50 ± 0.45 U L$^{-1}$) was the most induced enzyme followed by MnP (961.50 ± 0.22 U L$^{-1}$) and LiP (840 ± 0.31 U L$^{-1}$). The induction of Lac was steady over the 5 days experimental period (Fig). However, the induction of LiP and MnP was initially low in the first 2 days which later peaked by 530.50 ± 0.75 and 732.50 ± 0.53 U L$^{-1}$ at day 3 respectively. The two-way ANOVA revealed that induction of each enzymes was significantly different with respect to experimental time. These findings revealed that increased enzyme activities resulted in the removal of fluorene. Hence, fluorene degradation rate and efficiency were mediated by secretion of ligninolytic enzymes by *M. irregularis*. In recent times, Lac, LiP and MnP have been recognized to be significantly induced during microbial degradation of polycyclic aromatic hydrocarbons (Hadibarata and Kristanti, 2012). Laccase has been implicated in the degradation of several PAHs by many researchers (Dean-Ross and Cerniglia, 1996). Bressler et al. (2000) reported that laccase was responsible for the breakdown of fluorene to 9-fluorenone. However, in this present study, laccase was found to play a major role in the biodegradation mechanism and final breakdown of fluorene to phenol. The enzymes are involved in the mechanistic and oxidative activities involving ring cleavage, carboxylation and decarboxylation of fluorene to different metabolites. It is postulated that the catalytic nature of few peroxidase is due to a hybrid molecular architecture combining different substrate binding and oxidation sites (Wu et al., 2010).

### 3.5. Validation through growth linked degradation experiments after process optimization and confirmatory tests

Fluorene degradation pattern was studied with all the variables at their optimized levels (Figs. SM1 and 2f). Fig. 4 illustrates the enhanced degradation (82.50 ± 0.5%) and growth of *M. irregularis* within 5 days. It is noteworthy that the percentage degradation rate recorded in the validation experiment is quite close to the predicted degradation efficiency (81.50%) obtained during optimization of process parameters using BBD. The two-way ANOVA revealed that there was statistical difference between the growth of *M. irregularis* and fluorene degradation. The results also showed strong agreement between the two experiments. Hence, the Box–Behnken design used in the current study is

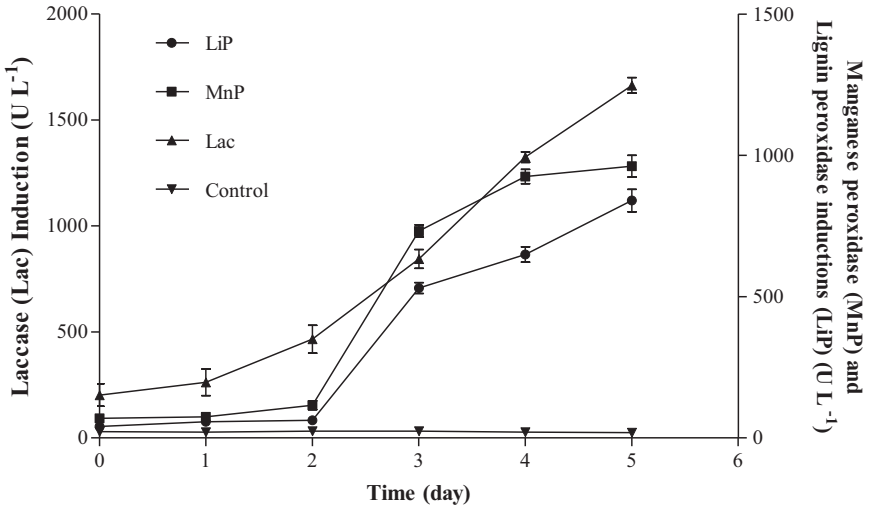


**Fig. 3.** Induction of enzymes during fluorene degradation by *M. irregularis*.

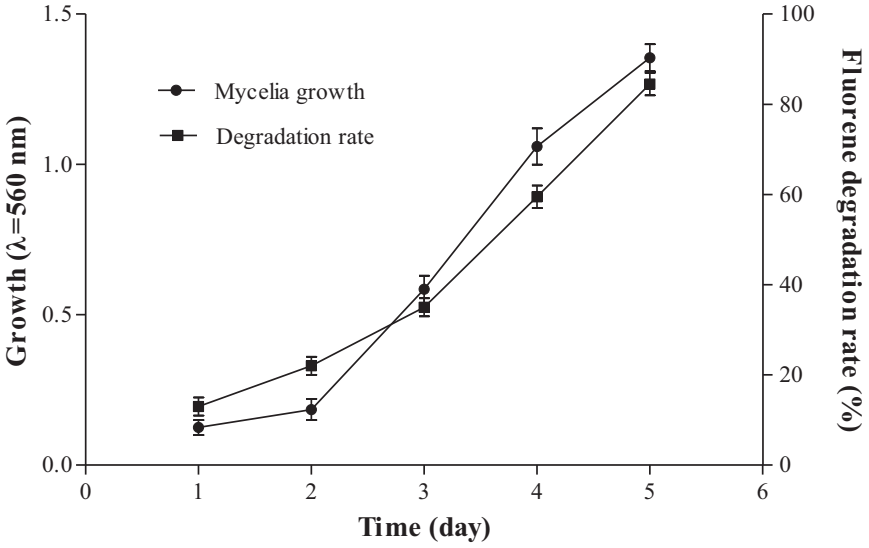


**Fig. 4.** Growth-linked enhanced fluorene degradation pattern with optimized levels of variables.

appropriate for optimized and enhanced prediction of fluorene degradation by *M. irregularis*.

## 4. Conclusions

The study is the first report of fluorene degradation by marine derived, *M. irregularis*. The RSM-BBD confirmed the interactive effect of pH, substrate concentration, dry weight and temperature on optimum degradation of fluorene by the fungus. It is noticeable that fungal mycelia dry weight, pH and concentration play a huge role in the degradation of fluorene. The BBD was found to be statistically significant with $p < 0.0001$, $F = 202.39$, predicted $R^2$ (0.9991) and adjusted $R^2$ (0.9980). Maximum degradation efficiency (81.50%) was achieved under optimal conditions. The optimization of vital media components resulted in 79.80% in fluorene degradation depletion by *M. irregularis*. The study revealed the influence of glucose and manganese ions in the enhanced degradation of fluorene by the fungus. The degradation mechanism and rate were improved with significant induction of laccase and manganese peroxidase. The study affirmed the promising potentials of marine derived *M. irregularis* in the degradation PAHs.

## CRediT authorship contribution statement

**Paul Olusegun Bankole:** Conceptualization, Experimental design, Methodology, Statistical analysis, Writing - original draft. **Kirk Taylor Semple:** Writing - review & editing. **Byong-Hun Jeon:** Revision, Vetting, Writing - review & editing. **Sanjay Prabhu Govindwar:** Writing - review & editing.

## Declaration of Competing Interest

The authors hereby declare no conflict of interest.

## Acknowledgements

Paul Olusegun Bankole hereby express profound thanks to the Association of Commonwealth Universities (ACU) for the 2019 Blue Charter Fellowship Award and the management of Federal University of Abeokuta, Ogun State, Nigeria for the institutional support.

## Appendix A. Supporting information

Supplementary data associated with this article can be found in the online version at doi:10.1016/j.ecoenv.2020.111619.

## References

Abdelhay, A., Magnin, J.P., Gondrexon, N., Baup, S., Willison, J., 2008. Optimization and modelling of phenanthrene degradation by *Mycobacterium* sp. 6PY1 in a biphasic medium using response-surface methodology. Appl. Microbiol. Biotechnol. 78, 881–888.

Ahearn, D.G., Meyers, S.P., 1972. The role of fungi in the decomposition of hydrocarbons in the marine environment. In: Walters, A.H., Hueck-van der Plas, E.H. (Eds.), Biodeterioration of Materials. Applied Science, London, 12–18.16.

Al-Hawash, A.B., Alkooranee, J.T., Zhang, X., Ma, F., 2018. Fungal degradation of polycyclic aromatic hydrocarbons. Int. J. Pure Appl. Biosci. 6 (2), 8–24. https://doi.org/10.18782/2320-7051.6302.

Archibald, F.S., 1992. A new assay for lignin type peroxidase employing the dye Azure B. Appl. Environ. Microbiol. 58, 3110–3116.

Bhatt, J.K., Ghevariya, C.M., Dudhagara, D.R., Rajpara, R.K., Dave, B.P., 2014. Application of response surface methodology for rapid chrysene biodegradation by newly isolated marine-derived fungus *Cochliobolus lunatus* strain CHR4D. J. Microbiol. 52 (11), 908–917.

Birolli G., W., de A Santos, D., Alvarenga, N., Garcia, A.C.F.S., Romão, L.P.C., Porto, A.L. M., 2018. Biodegradation of anthracene and several PAHs by the marine-derived fungus *Cladosporium* sp. CBMAI 1237. Mar. Pollut. Bull. 129 (2), 525–533. https://doi.org/10.1016/j.marpolbul.2017.10.023.

Bogan, B.W., Lamar, R.T., 1995. One-electron oxidation in the degradation of creosote polycyclic aromatic hydrocarbons by *Phonerochaete chrysosporiurn*. Appl. Environ. Microbiol. 61 (7), 2631–2635.

Bressler, D.C., Fedorak, P.M., Pickard, M.A., 2000. Oxidation of carbazole, N-ethylcarbazole, fluorene, and dibenzothiophene by the laccase of *Coriolopsis gallica*. Biotechnol. Lett. 22, 1119–1125.

Crampon, M., Bureau, F., Akpa-Vinceslas, M., Bodilis, J., Machour, N., Le Derf, F., 2014. Correlations between PAH bioavailability, degrading bacteria, and soil characteristics during PAH biodegradation in five diffusely contaminated dissimilar soils. Environ. Sci. Pollut. Res. Int. 21, 8133–8145. https://doi.org/10.1007/s11356-014-2799-6.

Czaplicki, L.M., Dharia, M., Cooper, E.M., Lee Ferguson, P., Gunsch, C.K., 2018. Evaluating the mycostimulation potential of select carbon amendments for the degradation of a model PAH by an ascomycete strain enriched from a superfund site. Biodegradation 29, 463–471. https://doi.org/10.1007/s10532-018-9843-z.

Das, A., Mishra, S., 2017. Removal of textile dye reactive Green-19 using bacterial consortium: process optimization using response surface methodology and kinetics study. J. Environ. Chem. Eng. 5 (1), 612–627. https://doi.org/10.1016/j.jece.2016.10.005.

Dean-Ross, D., Cerniglia, C.E., 1996. Degradation of pyrene by *Mycobacterium flavescens*. Appl. Microbiol. Biotechnol. 46, 307–312.

EPA, 2016. Priority chemicals. ⟨https://archive.epa.gov/epawaste/hazard/wastemin/web/html/priority.html⟩. (Accessed 10 December 2017).

Fu, Y., Viraraghavan, T., 2001. Fungal decolorization of dye wastewaters: a review. Bioresour. Technol. 79, 251–262.

Ghevariya, C.M., Bhatt, J.K., Dave, B.P., 2011. Enhanced chrysene degradation by halotolerant *Achromobacter xylosoxidans* using Response Surface Methodology. Bioresour. Technol. 102, 9668–9674. https://doi.org/10.1016/j.biortech.2011.07.069.

Griffith, G.W., Ozkose, E., Theodorou, M.K., Davies, D.R., 2009. Diversity of anaerobic fungal populations in cattle revealed by selective enrichment culture using different carbon sources. Fungal Ecol. 2, 87–97.

Hadibarata, T., Kristanti, R.A., 2012. Fate and cometabolic degradation of benzo[a] pyrene by white-rot fungus *Armillaria* sp. F022. Bioresour. Technol. 107, 314–318.

Hadibarata, T., Tachibana, S., 2009. Bioremediation of phenanthrene, chrysene, and benzo[a]pyrene by fungi screened from nature. ITB J. Sci. 41A (2), 88–97.

Haritash, A.K., Kaushik, C.P., 2009. Biodegradation aspects of Polycyclic Aromatic Hydrocarbons (PAHs): a review. J. Hazard. Mater. 169 (1–3), 1–15.2.

Hidayat, A., Yanto, D.H.Y., 2018. Biodegradation and metabolic pathway of phenanthrene by a new tropical fungus, *Trametes hirsuta* D7. J. Environ. Chem. Eng. 6 (2), 2454–2460. https://doi.org/10.1016/j.jece.2018.03.051.

Ike, P.T.L., Birolli, W.G., dos Santos, D.M., Porto, A.L.M., Souza, D.H.F., 2019. Biodegradation of anthracene and different PAHs by a yellow laccase from *Leucoagaricus gongylophorus*. Environ. Sci. Pollut. Res. 26 (9), 8675–8684. https://doi.org/10.1007/s11356-019-04197-z.

Isaac, P., Alessandrello, M.J., Macedo, A.J., Estévez, M.C., Ferrero, M.A., 2017. Pre-exposition to polycyclic aromatic hydrocarbons (PAHs) enhance biofilm formation and hydrocarbon removal by native multi-species consortium. J. Environ. Chem. Eng. 5, 1372–1378. https://doi.org/10.1016/j.jece.2017.b02.031.

Johannes, C., Majcherczyk, A., 2000. Natural mediators in the oxidation of polycyclic aromatic hydrocarbons by laccase mediator systems. Appl. Environ. Microbiol. 66, 524–528.

Johnsen, A.R., Wick, L.Y., Harms, H., 2005. Principles of microbial PAH-degradation in soil. Environ. Pollut. 133, 71–84.

Kim, J.D., Shim, S., Lee, C., 2005. Degradation of phenanthrene by bacterial strains isolated from soil in oil refinery fields in Korea. J. Microbiol. Biotechnol. 15, 337–345.

Kumar, S., Stecher, G., Li, M., Kynaz, C., Tamura, K., 2018. MEGA X: Molecular Evolutionary Genetics Analysis across Computing Platforms. Mol. Biol. Evol. 35 (6), 1547–1549. https://doi.org/10.1093/molbev/msy096.

Lee, H., Jang, Y., Choi, Y.-S., Kim, M.-J., Lee, J., Lee, H., Hong, J.-H., Lee, Y.M., Kim, G.-H., Kim, J.-J., 2014. Biotechnological procedures to select white rot fungi for the degrdadatio on PAHs. J. Microbiol. Methods 97, 56–62.

Mishra, S., Maiti, A., 2019. Effectual bio-decolourization of anthraquinone dye reactive blue-19 containing wastewater by *Bacillus cohnii* LAP217: process optimization. Bioremediation J. 24 (1), 1–20. https://doi.org/10.1080/10889868.2019.1671793.

Mohana, S., Shrivastava, S., Divecha, J., Madamwar, D., 2008. Response surface methodology for optimization of medium for decolorization of textile dye Direct Black 22 by a novel bacterial consortium. Bioresour. Technol. 99, 562–569.

Patnaik, P., 2007. A Comprehensive Guide to the Hazardous Properties of Chemical Substances. John Wiley & Sons. Inc. Publication.

Raghukumar, C., D'Souza-Ticlo, D., Verma, A., 2008. Treatment of colored effluents with lignin-degrading enzymes: an emerging role of marine-derived fungi. Crit. Rev. Microbiol. 34 (3–4), 189–206, 3.

Romero, M.C., Urrutia, M.I., Reinoso, H.E., Moreno Kiernan, M., 2010. Benzo[a]pyrene degradation by soil filamentous fungi. J. Yeast Fungal Res. 1, 25–29.

Sandhu, D.K., Arora, D.S., 1985. Laccase production and wood degradation of white rot fungus *Daedalea flavida*. Enzym. Microb. Technol. 7, 405–408.

Sandrin, T.R., Maier, R.M., 2003. Impact of metals on the biodegradation of organic pollutants. Environ. Health Perspect. 111, 1093–1101.

Santos, E.C., Jacques, J.S.R., Bento, M.F., Peralba, R.M.C., Selbach, P.A., 2008. Anthracene biodegradation and surface activity by an iron-stimulated *Pseudomonas* sp. Bioresour. Technol. 99, 2644–2649.

Simarro, R., González, N., Bautista, L.F., Monila, M.C., Schiavi, E., 2012. Evaluation of the influence of multiple environmental factors on the biodegradation of dibenzofuran, phenanthrene, and pyrene by a bacterial consortium using an orthogonal experimental design. Water Air Soil Pollut. 223, 3437–3444.

Sutar, S.S., Patil, P.J., Tamboli, A.S., Patil, D.N., Apine, O.A., Jadhav, J.P., 2019. Biodegradation and detoxification of malachite green by a newly isolated bioluminescent bacterium *Photobacterium leiognathi* strain MS under RSM optimized culture conditions. Biocatal. Agric. Biotechnol. 20, 101183.

Tamura, K., Nei, M., Kumar, S., 2004. Prospects for inferring very large phylogenies by using the neighbor-joining method. Proc. Natl. Acad. Sci. USA 101, 11030–11035.

Tang, Y.J., Krieger-Brockett, B., 2007. Mathematical analysis of the whole core injection method accuracy for measuring phenanthrene biodegradation rates in undisturbed marine sediments. Chemosphere 68, 804–813. https://doi.org/10.1016/j.chemosphere.2007.02.038.

Vieira, G.A.L., Magrini, M.J., Bonugli-Santos, R.C., Rodrigues, M.V.N., Sette, L.D., 2018. Polycyclic aromatic hydrocarbons degradation by marine-derived basidiomycetes: optimization of the degradation process. Braz. J. Microbiol. 49 (4), 749–756. https://doi.org/10.1016/j.bjm.2018.04.007.

Wu, Y.-R., Luo, Z.-H., Vrijmoed, L.L.P., 2010. Biodegradation of anthracene and benz [a] anthracene by two *Fusarium* ***solani*** strains isolated from mangrove sediments. Bioresour. Technol. 101, 9666–9672.

Xu, Y., Lu, M., 2010. Bioremediation of crude oil-contaminated soil: comparison of different biostimulation and bioaugmentation treatments. J. Hazard. Mater. 183, 395–401.

Zafra, G., Absalón, A.E., Cortés-Espinosa, D.V., 2015. Morphological changes and growth of filamentous fungi in the presence of high concentrations of PAHs. Braz. J. Microbiol. 46, 937–941.